Inorganic Chemistry

pubs.acs.org/IC

Featured Article

Selective and Efficient Biomacromolecular Extraction of Rare-Earth Elements using Lanmodulin

Gauthier J.-P. Deblonde,* Joseph A. Mattocks, Dan M. Park, David W. Reed, Joseph A. Cotruvo, Jr.,* and Yongqin Jiao

Cite This: *Inorg. Chem.* 2020, 59, 11855−11867

Read Online

ACCESS | Metrics & More | Article Recommendations | Supporting Information

ABSTRACT: Lanmodulin (LanM) is a recently discovered protein that undergoes a large conformational change in response to rare-earth elements (REEs). Here, we use multiple physicochemical methods to demonstrate that LanM is the most selective macromolecule for REEs characterized to date and even outperforms many synthetic chelators. Moreover, LanM exhibits metal-binding properties and structural stability unseen in most other metalloproteins. LanM retains REE binding down to pH ≈ 2.5, and LanM-REE complexes withstand high temperature (up to 95 °C), repeated acid treatments, and up to molar amounts of competing non-REE metal ions (including Mg, Ca, Zn, and Cu), allowing the protein's use in harsh chemical processes. LanM's unrivaled properties were applied to metal extraction from two distinct REE-containing industrial feedstocks covering a broad range of REE and non-REE concentrations, namely, precombustion coal and electronic waste leachates. After only a single all-aqueous step, quantitative and selective recovery of the REEs from all non-REEs initially present (Li, Na, Mg, Ca, Sr, Al, Si, Mn, Fe, Co, Ni, Cu, Zn, and U) was achieved, demonstrating the universal selectivity of LanM for REEs against non-REEs and its potential application even for industrial low-grade sources, which are currently underutilized. Our work indicates that biosourced macromolecules such as LanM may offer a new paradigm for extractive metallurgy and other applications involving f-elements.

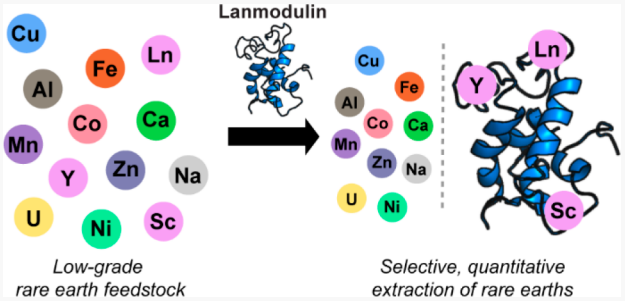

INTRODUCTION

Rare-earth elements (REEs) are essential to key sectors in the modern economy such as the electronic, energy, pharmaceutical, automobile, and military industries, but their supply chain is infamously monopolistic. The chemical processes currently implemented to extract REEs, purify them against non-REE elements, and separate them from each other are technically complex and environmentally detrimental.[1,2] Common hydrometallurgical methods such as solvent extraction or resin extraction require high-grade REE feedstocks. Classic techniques leverage small molecules (referred to as extractants or ligands) to extract the REEs, but their selectivity is usually limited (vide infra), which prevents their application to highly variable or diluted REE resources such as electronic waste, REE-containing coals, mine tailings, or geothermal brines.[3,4] On the other side of the REE life cycle, where applications such as medical imaging and cancer therapies rely on REE complexes, there is also a growing demand for more selective and robust REE chelators.[5−9]

In this context, the emergence of biosourced or bioinspired chelators for selective REE sequestration could offer a new avenue toward a more sustainable REE sector. Leveraging biomolecules for metal extraction technologies is appealing, as most biochemical processes occur with quantitative yields, fast kinetics, and high selectivity and fidelity. However, filling the gap between REE scavenging technologies and natural macromolecules presents two main scientific challenges: (1) traditional metalloproteins exhibit poor selectivity for REEs[10,11] and (2) physicochemical conditions encountered in industrial settings are often more demanding than in the cellular environment in terms of pH, temperature, and the presence of competing elements at high concentrations, particularly unchelated calcium, magnesium, zinc, and copper ions.[4,12,13]

Nature uses proteins—such as calmodulin for calcium,[14,15] vanabins for vanadium,[16,17] or transferrin,[18,19] ferritin,[20] and siderocalin for iron[21−23]—to selectively sense, uptake, and store essential metal ions. Until very recently, the uptake of rare-earth elements (and actinides) by metalloproteins had only been studied via metal substitutions within proteins naturally tailored to bind s- and d-block metal ions. Several

Received: May 1, 2020
Published: July 20, 2020

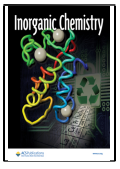

https://dx.doi.org/10.1021/acs.inorgchem.0c01303
Inorg. Chem. 2020, 59, 11855−11867

studies have shown that Fe^{3+}- or Ca^{2+}-binding proteins can be hijacked by trivalent lanthanide ions (Ln^{3+}) in vitro, but these proteins rarely encounter f-elements in their natural environments. However, the chemistry of 4f elements significantly differs from that of other blocks of the periodic table, with almost no redox chemistry under environmental conditions (except for the Ce^{4+}/Ce^{3+} couple[24]), a coordination number from 8 to 10 compared to the usual 4 to 6, and a large ionic radius (~1 Å[25]) relative to d-block metals. As such, while some natural proteins can tolerate distortions of the metal binding site and accommodate the voluminous Ln^{3+} ions under specific conditions,[14] they typically have lower affinity for the REEs than for the elements they have evolved to scavenge and transport. The dearth of naturally occurring, efficient REE-binding macromolecules has led the industry and associated research field to generally ignore proteins for the REE life cycle and favor small, man-made chelators instead.

The recent discovery that methylotrophic bacteria acquire and utilize certain lanthanides for essential biological functions has opened the possibility that natural and efficient REE-binding macromolecules might exist.[26−29] In 2018, lanmodulin (LanM, Scheme 1), a small protein of ~12 kDa produced by certain methylotrophic bacteria, was isolated and characterized as a natural, reversible REE-binding protein.[30]

Scheme 1. Representation of LanM (blue) Bound to Three REE Ions (cyan)[a]

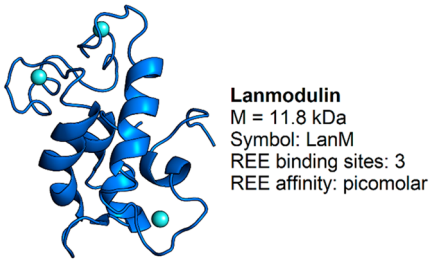

[a]The NMR solution structure of Y_3LanM (PDB code: 6MI5) has been reported elsewhere.[31]

LanM is the first identified macrochelator that has naturally evolved to reversibly sequester REE ions, motivating our investigation into its solution chemistry and potential use for industry-oriented applications. Previous studies[30,31] focused on LanM's characterization under physiological conditions (pH 7.2) and assessed metal binding indirectly via the protein's large conformational change. The present study offers direct experimental evidence, from several physicochemical techniques (including, to the best of our knowledge, the first use of weak 4f-4f visible transitions to directly monitor Ln^{3+} binding to a protein), that LanM forms highly stable and water-soluble complexes across the REE series over a wide pH range while retaining unprecedented selectivity against non-REE elements. Contrary to the REE-protein systems that have been studied so far, REE-LanM complexes were found to be remarkably resilient under acidic conditions, selective against molar concentrations of competing cations, and stable over a broad temperature range (up to 95 °C). Taken together, LanM's high solubility, extreme affinity, and selectivity for REEs as well as compatibility with industrial physicochemical conditions make it the most promising macromolecular candidate currently for applications targeting f-elements. Furthermore, we show that LanM enables one-step, quantitative extraction and purification of REEs from acid leachates of two industrially relevant feedstocks. These include electronic waste (E-waste) and precombustion coal (lignite), which are unsuitable for traditional extraction methods due to their low REE contents. The results demonstrate that biosourced macromolecules can outperform man-made chelators and may bring a paradigm shift to the highly constrained and nonsustainable methods currently used for REE extraction and purification.

RESULTS AND DISCUSSION

Solution Thermodynamics of LanM-REE Complexation. Initial characterization of LanM by circular dichroism (CD) spectroscopy in chelator-buffered REE solutions indicated that the protein undergoes a conformational change upon REE binding, with an apparent K_d value of ~5 to 25 pM across the lanthanide series, at pH 7.2.[30] Herein, the binding of trivalent REE ions to LanM was assessed directly by monitoring the 4f-4f absorbance bands of selected lanthanide ions using UV−visible−NIR (NIR = near-infrared) spectrophotometry. This technique has been used extensively for small REE-ligand complexes;[32,33] by contrast, metalloproteins have not been analyzed by this approach, to the best of our knowledge, likely due to the combination of low extinction coefficients of REE absorbance bands (<20 M^{-1} cm^{-1}) and solubility limitations of most proteins. We took advantage of the high solubility of LanM (>1 mM) and its three high-affinity REE binding sites[31,34] to investigate REE binding by UV−visible spectrophotometry (Figure S1). The fourth REE binding site in LanM has a $K_d \gg 1$ μM at pH 6.0, at least 5−6 orders of magnitude weaker than the other three sites,[30] and therefore it was not occupied under the titration conditions utilized in the present study.

Upon addition of LanM to solutions of Pr^{3+}, Nd^{3+}, Sm^{3+}, Dy^{3+}, Ho^{3+}, Er^{3+}, or Tm^{3+}, significant changes in the absorbance spectra were observed (Figure 1 and Figure S1). As absorption spectrophotometry probes the coordination sphere of the metal center, as opposed to the metal-induced protein conformational changes studied previously,[30] these spectral perturbations allow us to directly assess metal-protein binding. The absorption bands of the LanM-bound REEs were red-shifted by several nanometers compared to the free ions, indicating a strong stabilization of the Ln^{3+} ions by the protein (Table S1). A general broadening of the absorption bands was also observed (Figure S1), which corroborates the presence of multiple metal centers with similar coordination environment and lower symmetry compared to the free ions. This observation is supported by the solution-state NMR structure determined for the Y^{3+}-LanM system at neutral pH, in which three metal binding sites were observed.[31]

The global formation constants corresponding to the three tight binding sites of LanM (REE_3LanM − log β_{31}) were determined under mild acidic conditions (pH 5)—which are relevant to industrial REE extraction processes—using ethylenediaminetetraacetic acid (EDTA) as competing ligand. The REE-EDTA complexes possess spectral signatures sufficiently distinct from their LanM counterparts to allow for accurate monitoring of the ligand-exchange reactions, as exemplified for the Nd^{3+}-LanM-EDTA system in Figure 1. Excess EDTA (5−10 equiv relative to LanM) was found necessary to completely displace the Ln^{3+} ions from the protein, highlighting LanM's high affinity for REEs even under mildly acidic conditions.

https://dx.doi.org/10.1021/acs.inorgchem.0c01303
Inorg. Chem. 2020, 59, 11855−11867

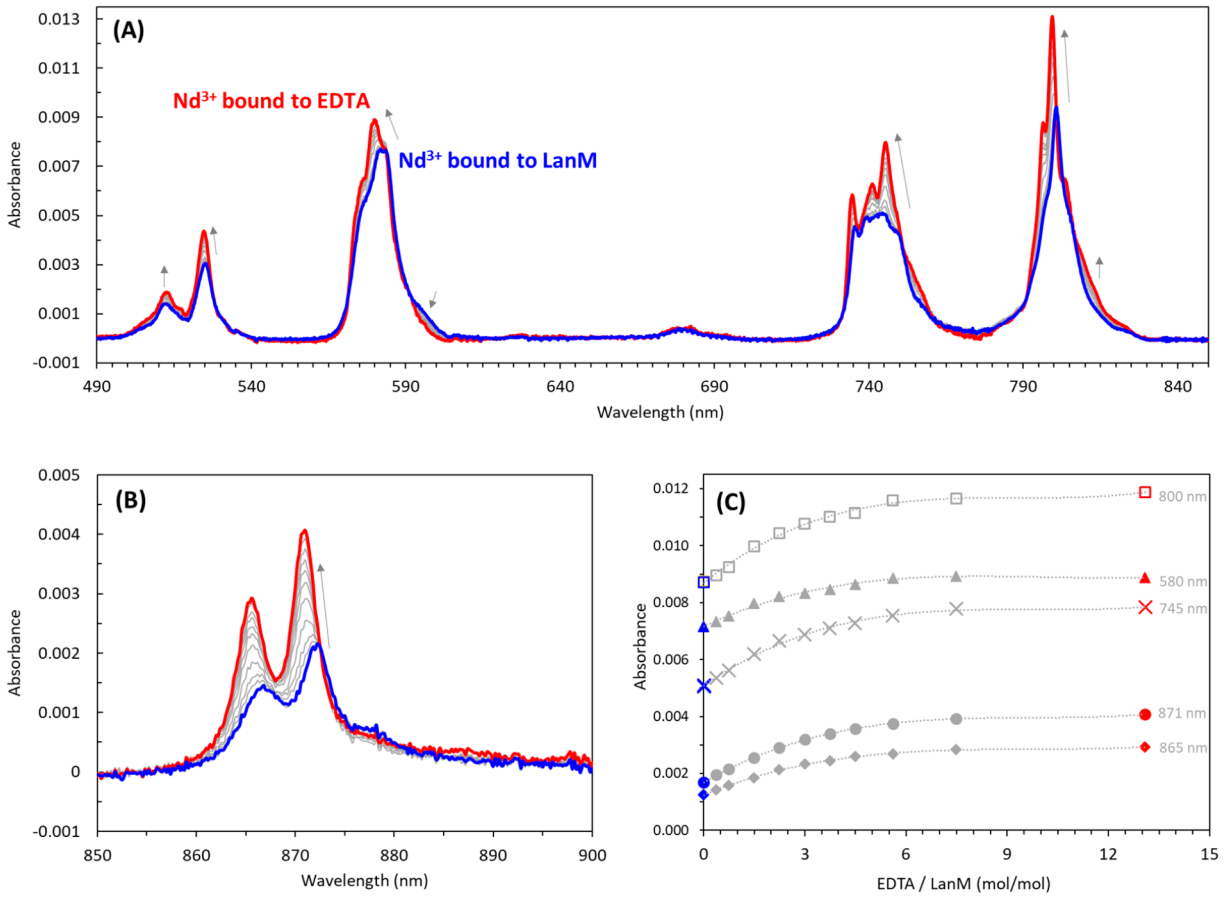

Figure 1. Competition between LanM and EDTA for REEs. Example of competition titration between LanM and EDTA for the binding to Nd^{3+} followed by UV−vis−NIR spectrophotometry. (A) 490−850 nm window. (B) 850−900 nm window. (C) Absorbance values for the most sensitive f-f absorbance bands. [Nd] = 1 mM. [LanM] = 0.31 mM. [EDTA] = 0 to 4.1 mM. pH = 5.0 (25 mM KCH_3COO, 75 mM KCl). T = 25 °C. The blue curves correspond to the initial sample (no EDTA), and the red ones correspond to the final sample (excess of EDTA). Arrows indicate the main spectral changes. Similar titrations were performed with Pr^{3+}, Sm^{3+}, Dy^{3+}, Ho^{3+}, Er^{3+}, and Tm^{3+} (Figure S2).

The kinetics of the ligand-exchange reactions was rapid (on the second to minute scale), allowing systematic investigation of all the REE-LanM systems suitable for UV−vis−NIR absorbance. Using the previously established stability constants of the REE-EDTA species as a reference,[35] refinement of the spectrophotometric data revealed that LanM forms exceptionally stable complexes across the REE series with global formation constants β_{31} between 10^{+32} and 10^{+37} (Table 1). Given the previous report[30] of LanM possessing three roughly equivalent metal binding sites, these formation constants correspond to an average K_d of 0.5−25 pM. The trend observed across the REE-LanM series departs from previously reported REE chelators such as the polyaminocarboxylates, which typically exhibit a continuous increase in affinity going from La^{3+} to Lu^{3+} (Figure S3). The trend observed in the case of LanM appears unique, as it is also opposite to that of previously studied lanthanide binding tags (LBTs) (Figure S4).

In addition, CD spectroscopy was used to monitor the REE-dependent conformational change in LanM at pH 5.0 in EDTA- or ethylene glycol-bis(β-aminoethyl ether)-*N*,*N*,*N*′,*N*′-tetraacetic acid (EGTA)-buffered solutions of representative REEs (Pr^{3+}, Gd^{3+}, Dy^{3+}, and Ho^{3+}), according to the previously described method[30] (Table 2 and Figure S5). These apparent K_d values range from 70 to 260 pM, only ∼10-fold weaker than the values obtained previously at pH 7.2 and similar to but slightly weaker than the K_d values determined from the spectrophotometric titrations focused on the REE absorbance bands. The differences may reflect distinct behavior of the protein in different concentration regimes (20 μM for CD vs 300−500 μM required for UV−vis−NIR) and/or a slight decoupling of metal binding and protein conformational change (which has been proposed in the case of Ca^{2+} binding to LanM[30]). It is interesting to note that these values match most closely for the biologically relevant, light REEs and deviate for heavy REEs, hinting that metal binding may not be the sole determinant of the protein's selective conformational response to REEs.[30,34] Regardless, these two independent methods demonstrate binding of REEs to LanM with picomolar affinity and remarkably similar K_d values across the entire lanthanide series.

In line with the K_d trend observed across the lanthanide series and the presence of multiple binding sites,[31] we also observed that LanM can scavenge heavy and light REEs (Pr^{3+} with Ho^{3+} or Er^{3+}) concomitantly upon its addition to a mixture of REEs (Figure S6). Likewise, REE-REE substitution assays also demonstrated LanM's ability to exchange one REE for another (Figure S7). The unusual similarity in affinity across the REE series can be leveraged to recover total REEs against the concomitant non-REE elements, provided that selectivity against the non-REEs is high (vide infra).

https://dx.doi.org/10.1021/acs.inorgchem.0c01303
Inorg. Chem. 2020, 59, 11855−11867

Table 1. Comparison of Metalloprotein and Synthetic Macromolecule Affinities (log β and K_d) for REEs. Binding Constants for Non-REE Ions and Corresponding Selectivity (K_d Ratio—Values Higher than 1 Indicate a Preference for the REEs) Are Also Given for Comparison. Additional Data Are Given in Table S2

macromolecule	metal binding reaction	log β	K_d	selectivity
lanmodulin	$3Pr^{3+} + LanM = Pr_3LanM$	32.9 ± 0.1[a]	10.6 pM[a]	
	$3Nd^{3+} + LanM = Nd_3LanM$	32.0 ± 0.1[a]	22.2 pM[a]	
	$3Sm^{3+} + LanM = Sm_3LanM$	31.9 ± 0.3[a]	24.2 pM[a]	
	$3Dy^{3+} + LanM = Dy_3LanM$	32.5 ± 0.3[a]	14.9 pM[a]	
	$3Ho^{3+} + LanM = Ho_3LanM$	33.2 ± 0.2[a]	8.58 pM[a]	
	$3Er^{3+} + LanM = Er_3LanM$	35.6 ± 0.2[a]	1.39 pM[a]	
	$3Tm^{3+} + LanM = Tm_3LanM$	37.2 ± 0.4[a]	0.41 pM[a]	
calmodulin	$Tb^{3+} + CaM = TbCaM$	5.3	5 μM[b]	
	$2Tb^{3+} + CaM = Tb_2CaM$	9.9	25 μM[b]	
	$3Tb^{3+} + CaM = Tb_3CaM$	14.6	20 μM[b]	
	$4Tb^{3+} + CaM = Tb_4CaM$	18.7	72 μM[b]	
				REE/Ca
	$Ca^{2+} + CaM = CaCaM$	4.5−6.4	0.37−34 μM[b′,b″]	0.07−6.8
	$2Ca^{2+} + CaM = Ca_2CaM$	8.1−12.8	0.46−245 μM[b′,b″]	0.02−9.8
	$3Ca^{2+} + CaM = Ca_3CaM$	11.8−18.6	1.6−185 μM[b′,b″]	0.08−9.3
	$4Ca^{2+} + CaM = Ca_4CaM$	14.9−23.6	8.5−814 μM[b′,b″]	0.12−11
ferritin	$Tb^{3+} + Ftn = TbFtn$	3.2−5.7[c]	2−666 μM	
transferrin	$Gd^{3+} + Tf = GdTf$	7.96[d]	11 nM	
	$2Gd^{3+} + Tf = Gd_2Tf$	13.9[d]	1148 nM	
				REE/Fe
	$Fe^{3+} + Tf = FeTf$	20.7[e]	2.1 × 10^{-21} M	1.9 × 10^{-13}
	$2Fe^{3+} + Tf = Fe_2Tf$	40.1[e]	4.2 × 10^{-20} M	3.7 × 10^{-14}
				REE/Cu
	$Cu^{2+} + Tf = CuTf$	12.3[f]	0.50 pM	4.6 × 10^{-5}
	$2Cu^{2+} + Tf = Cu_2Tf$	23.4[f]	7.9 pM	6.9 × 10^{-6}
siderocalin	$[Gd(Ent)]^{3-} + Scn = [Gd(Ent)]Scn$	8.3[g]	5.0 nM	REE/Fe
	$[Fe(Ent)]^{3-} + Scn = [Fe(Ent)]Scn$	9.4[g]	0.4 nM	0.08
lipocalin 2 mutants	$[Y(DTPA)]^{x-} + Lcn2 = [Y(DTPA)]Lcn2$	7.0−9.4[h]	0.4−88 nM	
LBT peptides	$Tb^{3+} + LBT = TbLBT$	7.2[i]	57 nM	
	$Tb^{3+} + dLBT = TbdLBT$	8.0−8.6[j]	2.5−10 nM	
	$2Tb^{3+} + dLBT = Tb_2dLBT$	15.5−16.2[j]	23−62 nM	

[a]UV−Vis spectrophotometry, pH 5.0, 100 mM KCl/KCH_3COO buffer (this work). [b]pH 6.8, 20 mM PIPES, 10 mM KCl.[11] [b′]pH 7.4, 10 mM TRIS, 10 mM KCl.[11] [b″]pH 7.55, 10 mM HEPES, 20 mM KCl.[37] [c]pH 6.5.[38] [d]pH 7.4 in the presence of 0.2 mM of synergistic bicarbonate, 100 mM HEPES buffer.[39,40] [e]pH 7.4 and atmospheric pCO_2.[41] [f]pH 7.4, 15 mM HCO_3^-.[10] [g]pH 7.4, HEPES buffer.[42] Ent = Enterobactin. [h]pH 8.8, 100 mM Tris, 100 mM NaCl, 5 mM $MgCl_2$. DTPA = Me·DTPA-RNase-DIG conjugate.[36] [i]pH 7.0, 10 mM HEPES, 100 mM NaCl.[43] [j]pH 7.0, 100 mM NaCl, 10 mM HEPES.[44]

Table 1 and Table S2 compare LanM with other metalloproteins previously studied for REE complexation—calmodulin (CaM), cadherin (Cad), S100β, ferritin (Ftn), transferrin (Tf), and siderocalin (Scn), as well as synthetic LBTs and double lanthanide binding tags (dLBTs). To the best of our knowledge, the strongest REE-binding macromolecules reported prior to LanM were variants of human lipocalin 2 (Lcn2) that were engineered by random mutagenesis to recognize a synthetic REE-DTPA (DTPA = diethylenetriaminepentaacetic acid) derivative with K_d values of 400 to ∼90 000 pM.[36]

Among small peptides engineered to bind Ln^{3+} ions, dLBT is the strongest, with one of its binding sites exhibiting a K_d of 2500 pM for Tb^{3+} (pH 7.0).[44] Therefore, even at the lower pH used in our studies (≤5.0), the affinity of LanM toward REEs is orders of magnitude higher than any lanthanide-binding macromolecule reported thus far.

Furthermore Tf, Lcn2, and Scn are unable to bind the metal ions directly, instead requiring a cochelator (also known as

https://dx.doi.org/10.1021/acs.inorgchem.0c01303
Inorg. Chem. 2020, 59, 11855−11867

Table 2. LanM-REE Apparent K_d Values as a Function of pH[a]

					selectivity		
	pH	$K_{d,app}$ (pM)	n	$\Delta[\theta]$	REE/Ca	REE/Cu	REE/Zn
Pr^{3+}	4.0	1900 ± 400[b]	2.9 ± 1.5	−900 ± 120	2.0 ± 10^7	7.6 ± 10^5	1.6 ± 10^7
	5.0	70 ± 10	2.8 ± 0.5	−980 ± 60			
	6.0	27 ± 11	3.7 ± 2.4	−1090 ± 160			
	7.2[c]	ND[d]	ND	ND			
Gd^{3+}	4.0	5400 ± 1000	1.9 ± 0.6	−970 ± 80	1.4 ± 10^7	5.3 ± 10^5	1.1 ± 10^7
	5.0	100 ± 10	2.5 ± 0.4	−900 ± 130			
	6.0	24 ± 2	3.4 ± 0.9	−1060 ± 140			
	7.2[c]	10 ± 4	2.8 ± 0.4	−1150 ± 80	7.1 ± 10^7		
Dy^{3+}	4.0	9200 ± 1200	2.8 ± 0.9	−890 ± 120	7.0 ± 10^6	2.7 ± 10^5	5.5 ± 10^6
	5.0	200 ± 50	2.6 ± 0.9	−980 ± 250			
	6.0	41 ± 4	3.4 ± 0.6	−1100 ± 140			
	7.2	ND	ND	ND			
Ho^{3+}	4.0	13000 ± 2000	2.9 ± 0.8	−920 ± 90	5.4 ± 10^6	2.0 ± 10^5	4.2 ± 10^6
	5.0	260 ± 60	2.7 ± 0.7	−970 ± 100			
	6.0	ND	ND	ND			
	7.2[c]	25 ± 4	2.4 ± 0.5	−1150 ± 90	2.8 ± 10^7		
Ca^{2+}	5.0	$(1.4 \pm 0.5) \pm 10^9$	1.1 ± 0.3	−650 ± 170			
	7.2[c]	$(7.1 \pm 0.3) \pm 10^8$	3.0 ± 0.2	−900 ± 10			
Cu^{2+}	5.0	$(5.3 \pm 1.3) \pm 10^7$	1.1 ± 0.5	−610 ± 120			
Zn^{2+}	5.0	$(1.1 \pm 0.5) \pm 10^9$	1.2 ± 0.6	−500 ± 250			

[a]Apparent K_d values (in pM), Hill coefficients (n), and change in molar ellipticity at 222 nm ($\Delta[\theta]$, deg cm^2 dmol^{-1} × 10^{-3}) from CD titrations of LanM with chelator-buffered solutions of selected Ln^{3+} ions, 20 °C. [b]Uncertainties were determined from standard deviations from two independent titrations. [c]From ref 30, 25 °C. [d]ND = not determined. Examples of raw CD titration data are given in Figure S5. Corresponding selectivity (K_d ratio) values are given for comparison with Table 1.

"synergistic anion"). For example, Tf only binds metal ions in the presence of excess bicarbonate,[39,40] citrate,[45] oxalate,[10] or nitrilotriacetate,[46] whereas Scn only binds cations that are already complexed to bacterial siderophore ligands such as enterobactin, catechols, and hydroxamates,[22,36] which restricts their potential use outside laboratory conditions. Unlike these proteins, LanM binds REEs directly. These comparisons indicate that LanM's high affinity and selectivity for REEs, without the need for a cochelator, make it a promising REE-binding protein not only under ideal laboratory conditions but also potentially in more complex, industry-relevant samples, motivating our further tests described below.

Selectivity against Non-REEs. The selectivity of REE chelators against non-REEs is of paramount importance for chelation-based separations due to the orders-of-magnitude higher concentrations of non-REEs in low-grade sources. Therefore, REE/non-REE substitutions were attempted with Nd^{3+}-LanM using Mg^{2+}, Ca^{2+}, Zn^{2+}, or Cu^{2+} as challengers. These competing elements were selected, because they are present at high concentrations (high μM range)[47,48] in environmental media as well as industrial feedstocks. Furthermore, the ionic radius of Ca^{2+} (1 Å)[25] is similar to that of the Ln^{3+} ions, and it is generally a strong competitor.

Samples containing 0.125 mM of Nd^{3+}-LanM were challenged by direct additions of concentrated $MgCl_{2(aq)}$, $CaCl_{2(aq)}$, $ZnSO_{4(aq)}$, or $CuCl_{2(aq)}$. As seen in Figure 2 and Figure S8, LanM retains its REE ions even in the presence of 1.5 M Mg^{2+}, 1.5 M Ca^{2+}, 0.4 M Zn^{2+}, or 10 mM Cu^{2+}. These concentrations exceed the impurity levels found in various low-grade sources, including end-of-life feedstocks containing REEs.[13,49] Since the intense blue absorption of Cu^{2+} precludes measurements at higher concentrations in our UV−vis−NIR method, the interactions between LanM and Cu^{2+} were also probed by CD. The apparent K_d for Cu-LanM is 53 μM at pH 5.0. Similar CD experiments with Zn^{2+} yielded an apparent K_d value of 1.1 mM at pH 5.0. These results further confirm LanM's poor affinity for Cu^{2+} and Zn^{2+} and its suitability for REE sources containing a large excess of non-REEs.

The performance of LanM in the presence of macroscopic amounts of impurities is unmatched by any other protein or LBT[50] (Table 1). Indeed, mammalian proteins such as Tf, Scn, and CaM exhibit affinity toward the REEs similar to or far lower than for their target elements in nature (Fe^{3+} and Ca^{2+}), which would translate into poor efficiency and selectivity for technologies aiming at REEs. By contrast, LanM is highly REE-selective, with its REE/non-REE relative binding affinity being at least 10^{+8} and 10^{+15} times higher than that of CaM and Tf, respectively (Table 1 and Table 2). For comparison, similar experiments were also performed with the synthetic and widely used polyaminocarboxylate chelator EDTA (Figure S9). Contrasting with the robustness and selectivity of LanM, EDTA releases its REE ions in the presence of ∼2 equiv of Zn^{2+} or Cu^{2+}.

Figure 3 benchmarks the thermodynamic selectivity Nd^{3+}/Zn^{2+} and Nd^{3+}/Cu^{2+} of LanM in comparison with that of various small chelators or macromolecules previously reported in the literature for REE applications. Supporting the experimental observations, the REE/non-REE selectivity of LanM is orders of magnitude higher than most small molecules or macromolecules ever studied. Therefore, not only is LanM the most REE-selective protein characterized to date and is able to retain REE binding in the presence of industrially relevant concentrations of competing ions; it is also more selective than synthetic small-molecule chelators.

Acid Tolerance and Thermal Stability. Most proteins denature under harsh physicochemical conditions such as those commonly encountered in hydrometallurgical processes, in particular, at low pH and high temperatures.[4,12] Contrary to

https://dx.doi.org/10.1021/acs.inorgchem.0c01303
Inorg. Chem. 2020, 59, 11855−11867

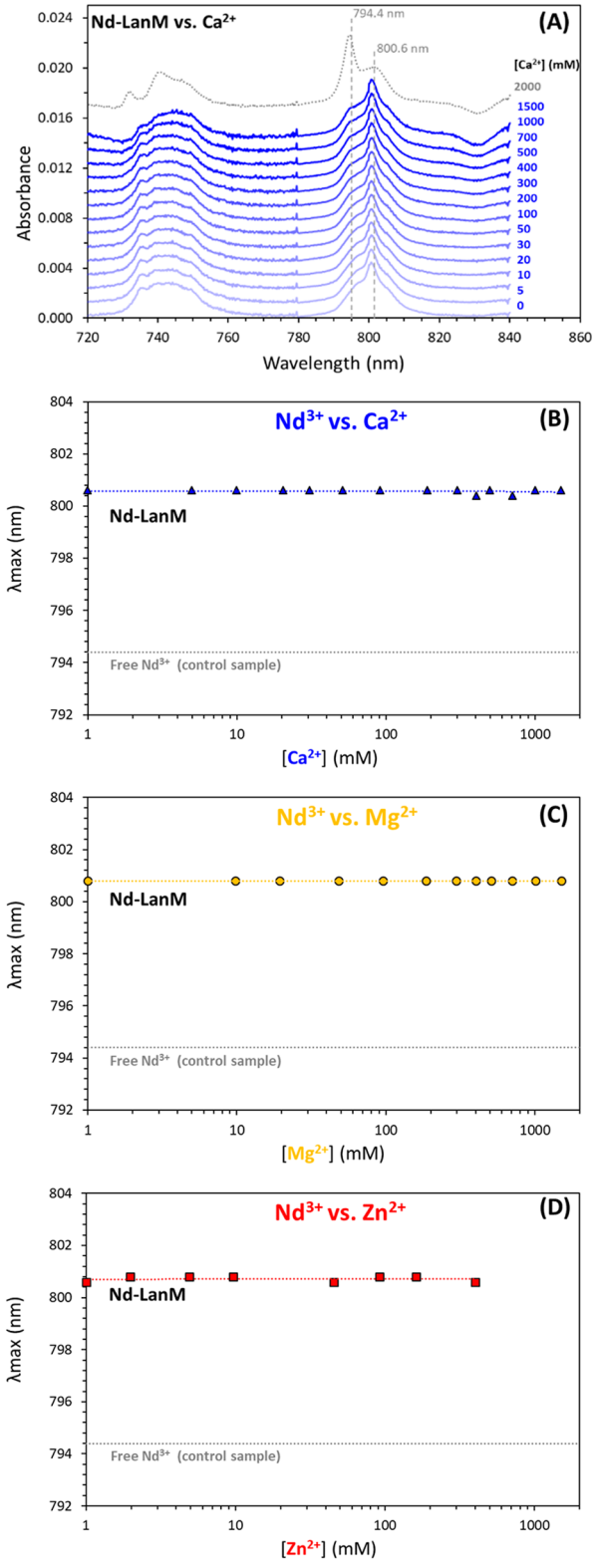

Figure 2. Robustness of REE-LanM complexes in Mg-, Ca-, and Zn-rich solutions. Competition assay between Nd^{3+}-LanM and Mg^{2+}, Ca^{2+}, or Zn^{2+}. [Nd] = 0.500 mM, [LanM] = 0.125 mM. Competitor: successive additions of $MgCl_2$, $CaCl_2$, or $ZnSO_4$. [Mg] = 0−1500 mM. [Ca] = 0−1500 mM. [Zn] = 0−400 mM. (A) Full UV−vis−NIR spectra of Nd-LanM in the presence of Ca^{2+}. (B−D) Wavelength of maximum absorbance (λ_{max}) as a function of the concentration of Ca^{2+}, Mg^{2+}, and Zn^{2+}, respectively. Buffer: 25 mM glycine, 25 mM KCH_3COO, 50 mM KCl, pH 5. Dotted curves: λ_{max} of control samples containing 0.500 mM $NdCl_3$ in the same buffer (no LanM). Similar results with Cu^{2+} and full absorbance spectra are given in Figure S8. Comparative experiments with EDTA instead of LanM are given in Figure S9.

other known REE-binding proteins, LanM was found to be remarkably tolerant of both conditions. First, REEs remain bound to LanM down to pH ≈ 2.5, as supported by multiple lines of physicochemical evidence including spectrophotometric titrations of REE-LanM solutions monitoring either the 4f-4f absorbance bands of LanM-bound REEs (Figure 4A and Figure S11) or the absorption of a tyrosine residue previously shown to be sensitive to Ln^{3+} ion binding and protein conformational change[30] (Figure S12). Similarly, dynamic light-scattering (DLS) experiments revealed a significant increase in the hydrodynamic diameter (from 3.5 to 5.5 nm) of the LanM-REE system below pH ≈ 2.5 (Figure 4B and Figure S13), suggesting the release of the REE ions and unfolding of the protein. This size change of LanM was confirmed to be directly correlated with REE binding (Figure S14). LanM's behavior at low pH was further confirmed by size-exclusion ultrafiltration and subsequent analysis of the filtrates (by both inductively coupled plasma mass spectrometry (ICP-MS) and Arsenazo III titrations; Figure 4C,D), which afford a direct confirmation of metal-protein complexation. Even in the micromolar range and with just a stoichiometric amount of LanM, REE ions remain bound to the protein down to pH ≈ 2.5. Circular dichroism titrations of LanM with a range of Ln^{3+} ions at acidic pH also indicated that the protein retains at least nanomolar affinity for REEs down to pH 4.0 (Table 2).

LanM's retention of REE binding at low pH contrasts sharply with previously studied REE-binding proteins, which release their metals under slightly subneutral pH. For example, although Tf has an extraordinarily high affinity toward Fe^{3+} (K_d ≈ 10^{-20} M) at neutral pH, it releases its metal ion at pH < 6.[51] Similarly, Scn is unable to retain its metal ions under acidic conditions.[52] The Fe^{3+}-siderophore-Scn adducts and most Fe^{3+}-siderophore complexes, which are among the most thermodynamically stable metal uptake mechanisms known in nature, are disrupted between pH 6 and 3.5.[52] Calmodulin, which shares some structural similarities with LanM, begins to release Ca^{2+} at ∼pH 6.[37] Synthetic LBTs are also unable to bind REEs below pH 5−6.[53]

LanM's affinity at low pH also compares favorably to common small-molecule chelators, such as EDTA and DTPA, which are widely used in analytical chemistry, nuclear chemistry, and pharmaceuticals.[7] These chelators protonate and release their REE ions at pH 2.5−3.0 (Figure S15), similarly to LanM, but they lack LanM's selectivity for REEs (Figure 3). LanM's combination of selectivity and performance at low pH challenges the general perception that man-made chelators are superior to or more robust than natural macromolecules.

The resilience of LanM to repeated acid attacks was also tested, given that acid desorption would be a convenient approach for REE recovery from the protein. Stoichiometric REE-LanM samples were first acidified to pH 1.8, left for 4 d, and then subjected to successive pH swing cycles below and above pH 2.5. As the LanM-bound and free REE ions have

https://dx.doi.org/10.1021/acs.inorgchem.0c01303
Inorg. Chem. 2020, 59, 11855−11867

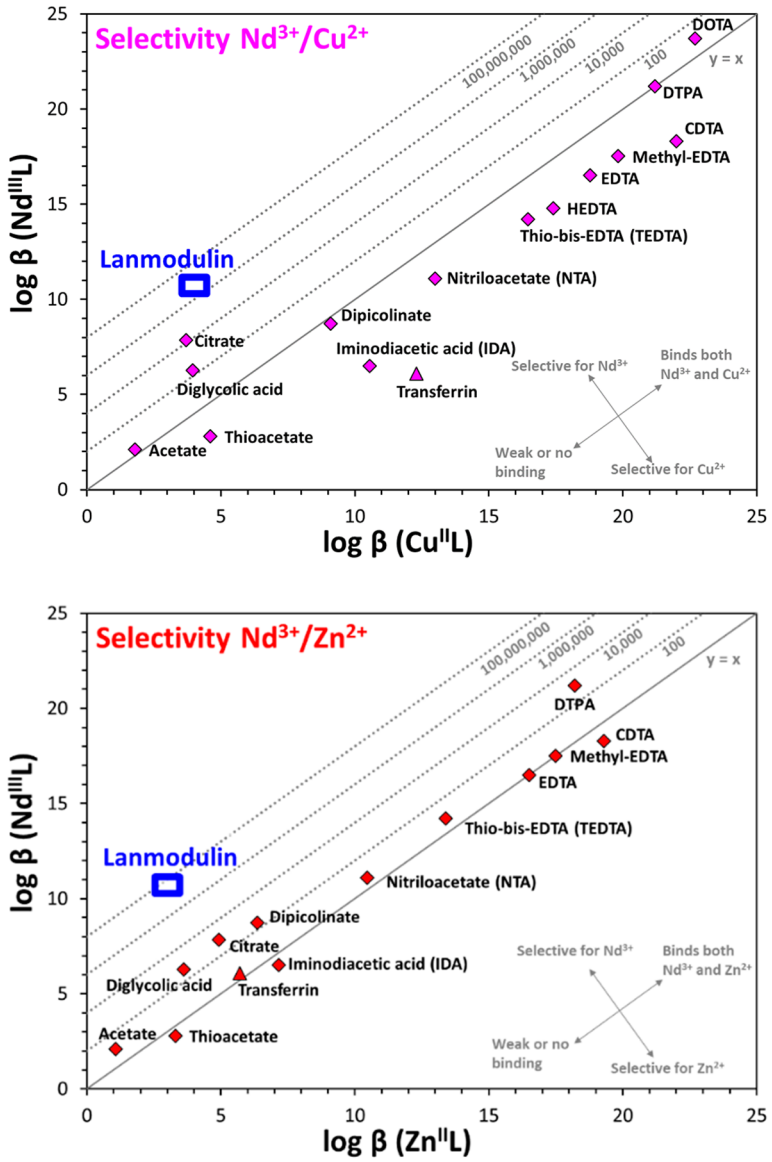

Figure 3. REE/Zn and REE/Cu thermodynamic selectivity of common REE chelators and comparison with LanM. Stability constants (log β) of 1:1 complexes of Nd^{3+} against Cu^{2+} (top) and Zn^{2+} (bottom) with various small-molecule chelators (◆) as well as transferrin (▲) and LanM (from Tables 1 and 2) for comparison. Data for the small chelators were taken from the NIST Critical database.[35] The full names and formulas of the chelators are given in Table S3. The dotted lines indicate a thermodynamic selectivity REE/non-REE of 10^{+2}, 10^{+4}, 10^{+6}, and 10^{+8}. The solid line $y = x$ corresponds to the absence of selectivity. The equivalent data for Nd^{3+}/Ca^{2+} selectivity is given in Figure S10.

distinct UV−vis−NIR absorbance signatures (Figure S1), the presence of unbound REE^{3+} or a change in the REE coordination environment would translate into spectral changes. As shown in Figure 5, no significant change is observed in the absorption spectrum of Nd-LanM and Er-LanM after multiple pH-triggered complexation and release cycles, indicating both the stability of LanM at low pH in the presence of REEs and the reversible binding of REE^{3+} ions to the protein. LanM also recovers REE binding following short-term exposure to even more acidic conditions (up to 1 M HCl), after it is brought back to pH > 2.5 (Figures S16 and S17). These results show that a potential industrial process comprising pH cycles above and below 2.5 offers a facile means of adsorbing and desorbing REEs while enabling protein recycling and reuse.

Thermal stability is also an important feature for many applications involving metal complexation. For example, geothermal fluids are an abundant but currently untapped source of REEs.[54] Since a temperature drop can lead to undesired mineral precipitation, mineral recovery from geothermal brines could benefit from a temperature-robust ligand for REE extraction. Most proteins are prone to denaturation, aggregation, and precipitation at high temperatures. By contrast, REE-LanM complexes were found to be highly thermally stable in solution. Stoichiometric Nd-LanM samples were subjected to an aggressive thermal treatment of 10 successive periods of 10 h from 25 to 95 °C. After this treatment, no change in the Nd^{3+}-LanM absorbance spectrum was detected, indicating that Nd^{3+} remained bound to LanM (Figure 6A).

Similar experiments using dynamic light scattering (30 min of incubation at each temperature) also indicate that both the REE-LanM and metal-free protein remain stable within the temperature range accessible in water at ambient pressure

https://dx.doi.org/10.1021/acs.inorgchem.0c01303
Inorg. Chem. 2020, 59, 11855−11867

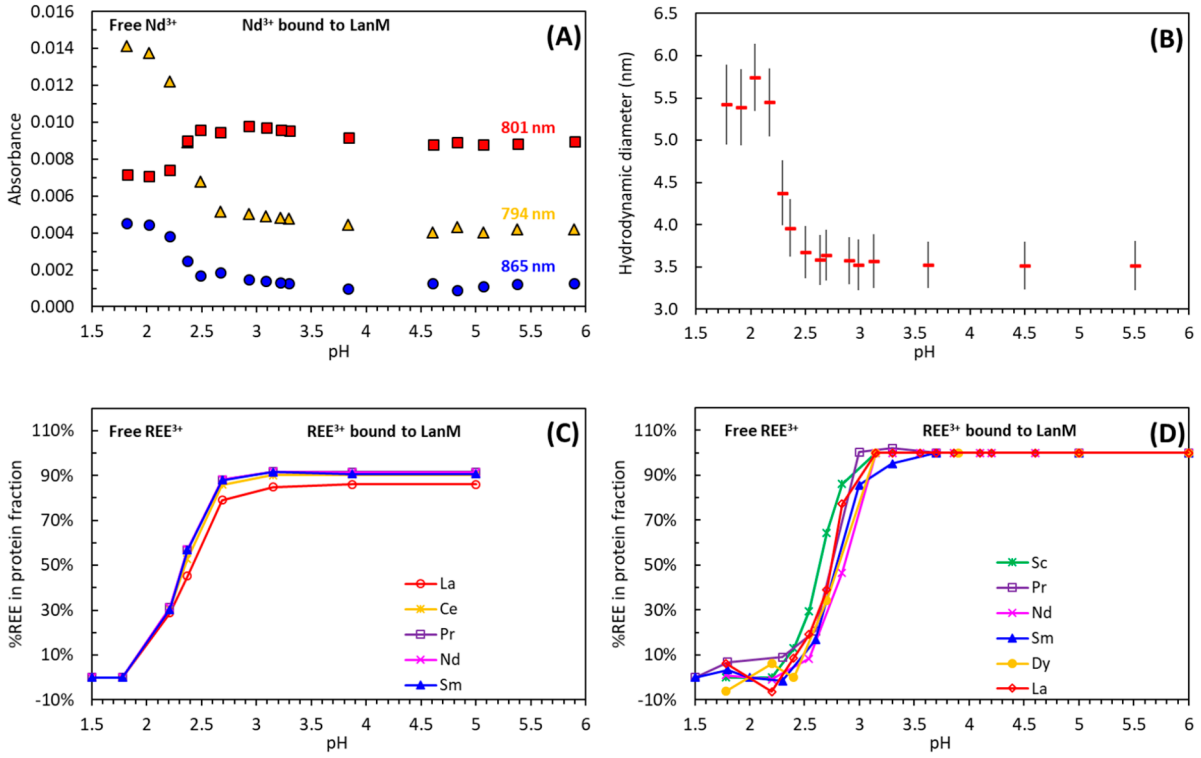

Figure 4. Stability of REE-LanM at low pH. Binding of REE^{3+} ions to LanM as a function of pH. (A) Primary spectral changes observed upon pH titration of Nd-LanM solutions. [Nd] = 1 mM. [LanM] = 0.25 mM. Buffer: 25 mM glycine, 25 mM KCH_3COO, 50 mM KCl. Full absorbance spectra and similar data obtained with Pr^{3+}, Er^{3+}, and Ho^{3+} are given in Figure S11. (B) Hydrodynamic diameter of Nd-LanM measured by DLS as a function of pH. [Nd] = 600 μM. [LanM] = 100 μM. T = 25 °C. The vertical black bars correspond to the average width of size distribution (eight measurements). The horizontal red rectangles represent the average size. Full DLS size distributions are given in Figure S13. (C) Size-exclusion ultracentrifugation of REE-LanM samples at as a function of pH using an equimolar mixture of REEs. $[REE]_{total}$ = 200 μM. [LanM] = 50 μM. Metal concentrations determined by ICP-MS. (**D**) Size-exclusion ultracentrifugation of REE-LanM samples as a function of pH using individual REE solutions at low concentrations. $[REE]_{initial}$ = 30 μM. [LanM] = 10 μM. Filtration performed with 3 kDa molecular weight cutoff spin filters. Metal concentrations determined by Arsenazo III assay.

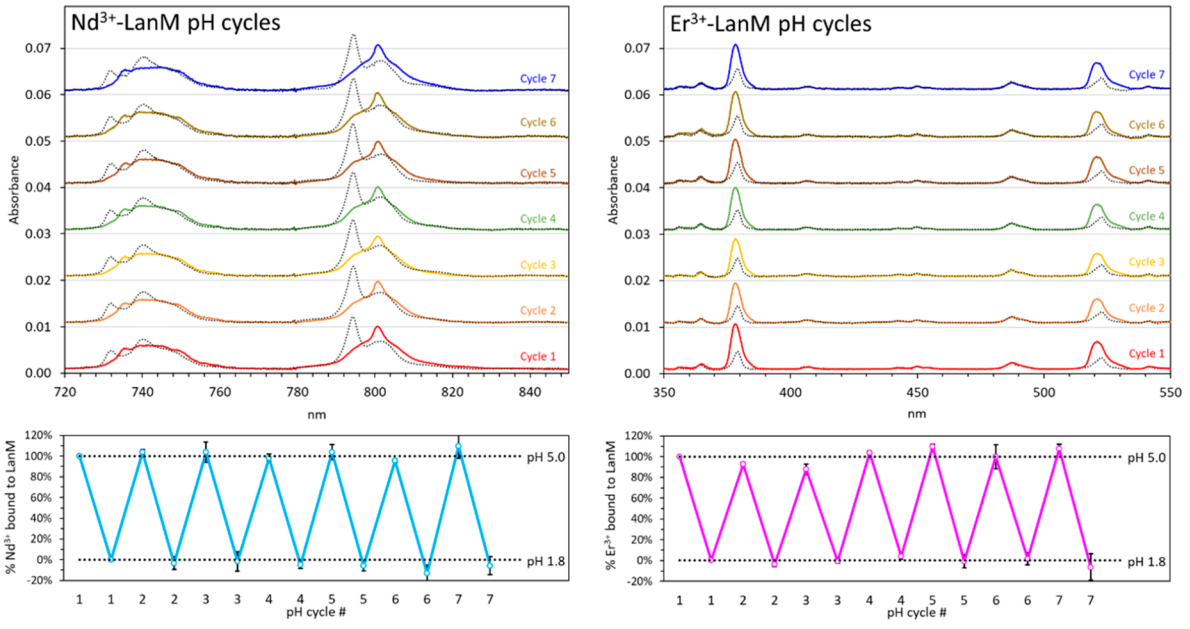

Figure 5. Resilience of LanM to repeated REE adsorption−desorption pH cycling. Absorbance spectra of Nd^{3+}-LanM (left) and Er^{3+}-LanM (right) systems following acid−base pH cycles (between pH 1.8 and 5). Solid curves: Ln^{3+} bound to LanM (pH > 2). Dotted curves: Ln^{3+} released from LanM (pH < 2). Spectra stacked for clarity. (bottom) %REE bound to LanM calculated based on the most sensitive absorbance wavelengths: 795 and 732 nm for Nd, 520 and 377 nm for Er.

https://dx.doi.org/10.1021/acs.inorgchem.0c01303
Inorg. Chem. 2020, 59, 11855−11867

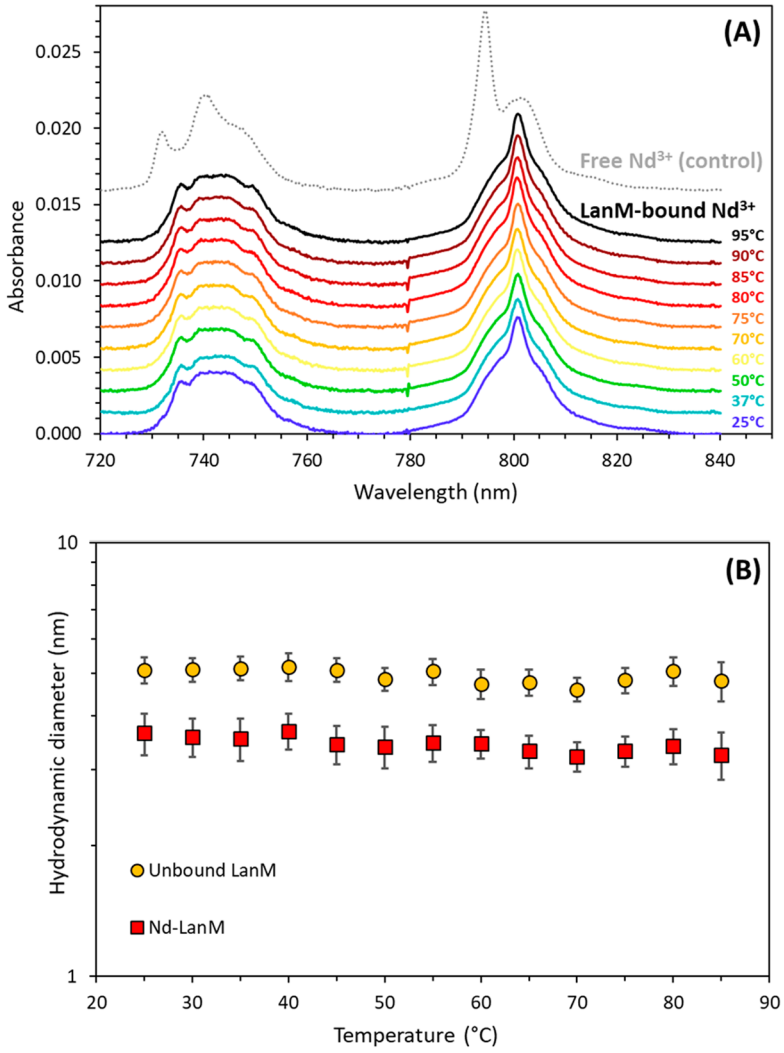

Figure 6. Thermal stability of REE-LanM. (A) UV−vis−NIR spectrophotometry of Nd^{3+}-LanM following incubation at various temperatures. [Nd] = 1 mM, [LanM] = 0.25 mM. Spectra are stacked for clarity. Dotted curve: 1 mM $NdCl_3$, no LanM. The samples were successively incubated for 10 h at each temperature from 25 to 95 °C as indicated next to each curve (total test >100 h). Absorbance spectra were measured after cooling of the samples to room temperature. Buffer: 25 mM glycine, 25 mM KCH_3COO, 50 mM KCl, pH 5. (B) Hydrodynamic diameter of unbound LanM and Nd-bound LanM measured by DLS. [LanM] = 100 μM. [Nd] = 0 or 600 μM. The samples were successively incubated for 30 min at each temperature from 25 to 85 °C. Buffer: 10 mM glycine, 10 mM KCH_3COO, pH 5.

(Figure 6B). The origin of the robust pH and thermal stability of the REE-LanM is currently unknown, but it may be related to the intrinsically disordered nature of the apoprotein.[30,55] These results highlight the robustness and resilience of the REE-LanM species and the suitability of this particular protein for applications necessitating harsh physicochemical conditions.

Performance Tests with Industrially Relevant Feedstocks. Finally, the unique properties of LanM were tested on industrial REE feedstocks. Precombustion coal (lignite) and electronic waste (E-waste) are abundant and potentially valuable REE sources that are currently unused.[13,56] These nonconventional sources are complex mixtures of REE and non-REE materials with a high composition variability compared to natural REE ores, and their processing would require a robust and versatile purification technology.[2] The metal ion concentrations in acid leachates (pH 3.7) of E-waste and lignite used in our experiments spanned over 3 orders of magnitude for the REEs (from ∼10 to 20 000 ppb) and 5 orders of magnitude for the non-REEs (from ∼100 to 3 000 000 ppb). Conventional chelators lack selectivity to efficiently extract and purify the REEs from such media (vide supra). As shown in Figure 7, even in acidic industrial matrixes with low REE content and large amounts of competing ions (Mg, Ca, Sr, Al, Si, Mn, Fe, Co, Ni, Cu, Zn, and U), LanM selectively scavenges the REEs while leaving behind all of the non-REE elements. A slight apparent selectivity for light over heavy REEs (Figures 7B,D) is more likely the result of higher initial concentrations of light REEs than heavy REEs, as the affinities of all REEs are relatively similar (Table 1). Direct addition of LanM to the leachates followed by a single size-exclusion filtration step affords an all-aqueous one-step process to selectively recover the REEs from complex and acidic industrial streams—transforming diluted, complex, and low-purity REE feedstocks into concentrated and purified REE streams. After a single step, the recovery yields for the lanthanides were greater than 99.5% in the case of the lignite and 99.8% for the E-waste (ICP-MS limit of quantification reached). Scandium and yttrium were recovered with a 96% yield under our experimental setting.

https://dx.doi.org/10.1021/acs.inorgchem.0c01303
Inorg. Chem. 2020, 59, 11855−11867

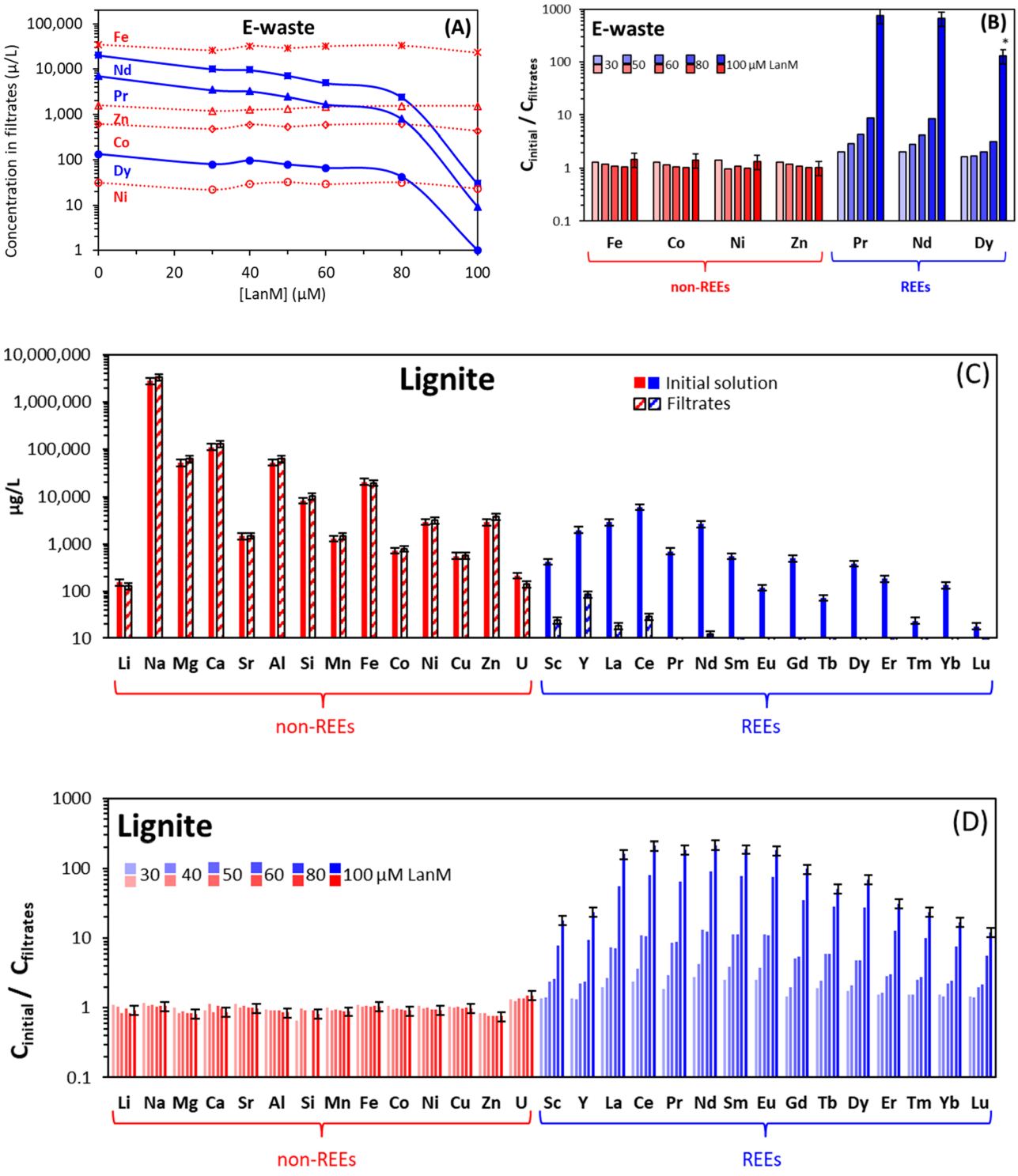

Figure 7. Protein-based selective recovery of REEs from industrial feedstocks. (A) Concentrations of REEs (blue curves) and non-REE impurities (red curves) in the low-molecular weight filtrates after addition of LanM to the electronic waste leachate, pH = 3.7, [LanM] = 0−100 μM. The corresponding linear scale figure is given in Figure S18. (B) Concentration ratios between the initial E-waste leachate solution and the filtrates. (C) Compositions of the initial lignite feedstock leachate (solid fill) and the low-molecular weight filtrates (pattern fill). [LanM] = 100 μM. pH = 3.7. (D) Concentration ratios between the initial lignite leachate solution and the filtrates. Metal concentrations were determined by ICP-MS (see Experimental Section for details). Ho was not analyzed to due to unresolved ICP-MS interferences. Error bars correspond to ±15%. This uncertainty (3σ) is conservative and takes into account the uncertainties of the experimental procedure and analytical protocol.

These results highlight LanM's unique affinity for the REEs and its minimal interaction with other natural elements across the periodic table. Common hydrometallurgical technologies, such as solvent extraction or precipitation, are not technically and economically viable for processing low-grade feedstocks due to their limited selectivity, low concentration factor per

https://dx.doi.org/10.1021/acs.inorgchem.0c01303
Inorg. Chem. 2020, 59, 11855−11867

purification step, and high environmental footprint.[3,4] Therefore, the development of a LanM-based extraction process could enable selective recovery of REEs from abundant but currently untapped REE resources. Work in progress to immobilize LanM onto solid supports would result in a more scalable REE purification system.

CONCLUSION

In summary, LanM's peerless behavior has been long sought for a metalloprotein for applications targeting REEs: it is highly selective toward REE ions even in the presence of high concentrations of non-REE cations, complexes with REEs at low pH, and is stable under acidic conditions and high temperatures. To the best of our knowledge, these properties of LanM are unmatched by any other known REE macrochelators and even outperform many synthetic chelators. Despite these extraordinary properties, the REE binding mode of LanM is relatively ordinary, with four to five carboxylate groups coming from aspartate and glutamate residues and one backbone carbonyl,[31] reminiscent of LBTs and polyaminocarboxylate ligands.[43,44] Therefore, effects beyond the local coordination environment of the metal ions likely drive the REE selectivity and stability of LanM.[31] The case of LanM opens a new front for developing protein-based REE extraction technologies that are highly selective, efficient, and versatile. Given LanM's affinity and selectivity for trivalent REEs, this protein and its potential derivatives also appear to be strong candidates for other applications targeting REEs and trivalent actinides such as gadolinium magnetic resonance imaging (MRI) contrast agents and radiopharmaceuticals based on actinium ($^{225}Ac^{3+}$) or REEs ($^{177}Lu^{3+}$, $^{149}Tb^{3+}$, $^{134}Ce^{3+}$, $^{90}Y^{3+}$, $^{44}Sc^{3+}$, etc.) as well as the environmental management of heavy actinides (Am^{3+}, Cm^{3+}, Bk^{3+}, etc.). Work is ongoing to evaluate the potential of LanM for actinide chemistry and to develop and utilize even more selective and resilient LanM variants for a range of applications from mining to medicine.

EXPERIMENTAL SECTION

Complete experimental details are provided in the Supporting Information.

ASSOCIATED CONTENT

Supporting Information

The Supporting Information is available free of charge at https://pubs.acs.org/doi/10.1021/acs.inorgchem.0c01303.

Full Experimental Section, supplementary experimental results (UV−vis−NIR and tyrosine absorbance spectrophotometric titrations of REE-LanM systems, circular dichroism titrations, dynamic light scattering measurements), literature data (REE-macromolecule thermodynamics, synthetic ligand formula, speciation diagrams), figures, tables, and references (PDF)

AUTHOR INFORMATION

Corresponding Authors

Gauthier J.-P. Deblonde − *Physical and Life Sciences Directorate and Glenn T. Seaborg Institute, Lawrence Livermore National Laboratory, Livermore, California 94550, United States;* orcid.org/0000-0002-0825-8714; Email: Deblonde1@llnl.gov

Joseph A. Cotruvo, Jr. − *Department of Chemistry, The Pennsylvania State University, University Park, Pennsylvania 16802, United States*; Email: juc96@psu.edu

Authors

Joseph A. Mattocks − *Department of Chemistry, The Pennsylvania State University, University Park, Pennsylvania 16802, United States;* orcid.org/0000-0003-1541-0187

Dan M. Park − *Physical and Life Sciences Directorate, Lawrence Livermore National Laboratory, Livermore, California 94550, United States*

David W. Reed − *Biological & Chemical Science & Engineering Department, Idaho National Laboratory, Idaho Falls, Idaho 83415, United States;* orcid.org/0000-0003-4877-776X

Yongqin Jiao − *Physical and Life Sciences Directorate, Lawrence Livermore National Laboratory, Livermore, California 94550, United States;* orcid.org/0000-0002-6798-5823

Complete contact information is available at: https://pubs.acs.org/10.1021/acs.inorgchem.0c01303

Author Contributions

G.J.-P.D., J.A.M., D.M.P., J.A.C., and Y.J. designed the research. G.J.-P.D., J.A.M., and D.M.P. collected experimental data. D.W.R. provided industrial feedstocks. All of the authors discussed the results and commented on the manuscript.

Notes

The authors declare the following competing financial interest(s): G.J.-P.D., J.A.M., D.M.P., J.A.C., and Y.J. are listed as inventors on patent applications filed by Lawrence Livermore National Laboratory and the Pennsylvania State University and describing inventions partially related to the research results presented here. The remaining authors declare no competing interests.

ACKNOWLEDGMENTS

This research was supported by the Critical Materials Institute (CMI), a Department of Energy (DOE) Innovation Hub led by the U.S. Department of Energy's Ames Laboratory and supported by the DOE's Office of Energy Efficiency and Renewable Energy's Advanced Manufacturing Office. CMI seeks ways to reduce supply risks on rare-earth metals and other materials critical to the success of clean energy technologies. This work was performed under the auspices of the U.S. DOE by Lawrence Livermore National Laboratory under Contract No. DE-AC52-07NA27344 (LLNL-JRNL-805884) and DOE Idaho Operations Office Contract No. DE-AC07-05ID14517. J.A.C. also thanks the Pennsylvania State University Department of Chemistry, Huck Institutes of Life Sciences, a Louis Martarano Career Development Professorship, and a Lab to Bench Commercialization Grant from Invent Penn State for funding. The authors thank A. Middleton, H. Hsu-Kim, S. Wang, and M. Gonzales for help with the ICP-MS analyses. The authors thank N. Theaker for providing lignite leachate solutions.

REFERENCES

(1) Izatt, R. M.; Izatt, S. R.; Bruening, R. L.; Izatt, N. E.; Moyer, B. A. Challenges to Achievement of Metal Sustainability in Our High-Tech Society. *Chem. Soc. Rev.* **2014**, *43* (8), 2451−2475.

(2) Cheisson, T.; Schelter, E. J. Rare Earth Elements: Mendeleev's Bane, Modern Marvels. *Science* **2019**, *363* (6426), 489−493.

(3) Xie, F.; Zhang, T. A.; Dreisinger, D.; Doyle, F. A Critical Review on Solvent Extraction of Rare Earths from Aqueous Solutions. *Miner. Eng.* **2014**, *56*, 10−28.
(4) Jha, M. K.; Kumari, A.; Panda, R.; Rajesh Kumar, J.; Yoo, K.; Lee, J. Y. Review on Hydrometallurgical Recovery of Rare Earth Metals. *Hydrometallurgy* **2016**, *165*, 2−26.
(5) McDevitt, M. R.; Thorek, D. L. J.; Hashimoto, T.; Gondo, T.; Veach, D. R.; Sharma, S. K.; Kalidindi, T. M.; Abou, D. S.; Watson, P. A.; Beattie, B. J.; Timmermand, O. V.; Strand, S.-E.; Lewis, J. S.; Scardino, P. T.; Scher, H. I.; Lilja, H.; Larson, S. M.; Ulmert, D. Feed-Forward Alpha Particle Radiotherapy Ablates Androgen Receptor-Addicted Prostate Cancer. *Nat. Commun.* **2018**, *9* (1), 1−11.
(6) Ferrier, M. G.; Batista, E. R.; Berg, J. M.; Birnbaum, E. R.; Cross, J. N.; Engle, J. W.; La Pierre, H. S.; Kozimor, S. A.; Lezama Pacheco, J. S.; Stein, B. W.; Stieber, S. C. E.; Wilson, J. J. Spectroscopic and Computational Investigation of Actinium Coordination Chemistry. *Nat. Commun.* **2016**, *7* (1), 1−8.
(7) Clough, T. J.; Jiang, L.; Wong, K.-L.; Long, N. J. Ligand Design Strategies to Increase Stability of Gadolinium-Based Magnetic Resonance Imaging Contrast Agents. *Nat. Commun.* **2019**, *10* (1), 1−14.
(8) Penfield, J. G.; Reilly, R. F. What Nephrologists Need to Know about Gadolinium. *Nat. Clin. Pract. Nephrol.* **2007**, *3* (12), 654−668.
(9) Nelson, J. J. M.; Cheisson, T.; Rugh, H. J.; Gau, M. R.; Carroll, P. J.; Schelter, E. J. High-Throughput Screening for Discovery of Benchtop Separations Systems for Selected Rare Earth Elements. *Commun. Chem.* **2020**, *3* (1), 1−6.
(10) Sun, H.; Li, H.; Sadler, P. J. Transferrin as a Metal Ion Mediator. *Chem. Rev.* **1999**, *99* (9), 2817−2842.
(11) Ye, Y.; Lee, H.-W.; Yang, W.; Shealy, S.; Yang, J. J. Probing Site-Specific Calmodulin Calcium and Lanthanide Affinity by Grafting. *J. Am. Chem. Soc.* **2005**, *127* (11), 3743−3750.
(12) Tunsu, C.; Petranikova, M.; Gergorić, M.; Ekberg, C.; Retegan, T. Reclaiming Rare Earth Elements from End-of-Life Products: A Review of the Perspectives for Urban Mining Using Hydrometallurgical Unit Operations. *Hydrometallurgy* **2015**, *156*, 239−258.
(13) Laudal, D. A.; Benson, S. A.; Addleman, R. S.; Palo, D. Leaching Behavior of Rare Earth Elements in Fort Union Lignite Coals of North America. *Int. J. Coal Geol.* **2018**, *191*, 112−124.
(14) Edington, S. C.; Gonzalez, A.; Middendorf, T. R.; Halling, D. B.; Aldrich, R. W.; Baiz, C. R. Coordination to Lanthanide Ions Distorts Binding Site Conformation in Calmodulin. *Proc. Natl. Acad. Sci. U. S. A.* **2018**, *115* (14), E3126−E3134.
(15) Kawasaki, H.; Soma, N.; Kretsinger, R. H. Molecular Dynamics Study of the Changes in Conformation of Calmodulin with Calcium Binding and/or Target Recognition. *Sci. Rep.* **2019**, *9* (1), 1−10.
(16) Costa Pessoa, J.; Garribba, E.; Santos, M. F. A.; Santos-Silva, T. Vanadium and Proteins: Uptake, Transport, Structure, Activity and Function. *Coord. Chem. Rev.* **2015**, *301*−*302*, 49−86.
(17) Hamada, T.; Asanuma, M.; Ueki, T.; Hayashi, F.; Kobayashi, N.; Yokoyama, S.; Michibata, H.; Hirota, H. Solution Structure of Vanabin2, a Vanadium(IV)-Binding Protein from the Vanadium-Rich Ascidian Ascidia Sydneiensis Samea. *J. Am. Chem. Soc.* **2005**, *127* (12), 4216−4222.
(18) Boradia, V. M.; Malhotra, H.; Thakkar, J. S.; Tillu, V. A.; Vuppala, B.; Patil, P.; Sheokand, N.; Sharma, P.; Chauhan, A. S.; Raje, M.; Raje, C. I. Mycobacterium Tuberculosis Acquires Iron by Cell-Surface Sequestration and Internalization of Human Holo-Transferrin. *Nat. Commun.* **2014**, *5* (1), 1−13.
(19) Holland, J. P.; Evans, M. J.; Rice, S. L.; Wongvipat, J.; Sawyers, C. L.; Lewis, J. S. Annotating MYC Status with 89 Zr-Transferrin Imaging. *Nat. Med.* **2012**, *18* (10), 1586−1591.
(20) Honarmand Ebrahimi, K.; Bill, E.; Hagedoorn, P.-L.; Hagen, W. R The Catalytic Center of Ferritin Regulates Iron Storage via Fe(II)-Fe(III) Displacement. *Nat. Chem. Biol.* **2012**, *8* (11), 941−948.
(21) Harris, W. R. Binding and Transport of Aluminum by Serum Proteins. *Coord. Chem. Rev.* **1996**, *149*, 347−365.
(22) Flo, T. H.; Smith, K. D.; Sato, S.; Rodriguez, D. J.; Holmes, M. A.; Strong, R. K.; Akira, S.; Aderem, A. Lipocalin 2 Mediates an Innate Immune Response to Bacterial Infection by Sequestrating Iron. *Nature* **2004**, *432* (7019), 917−921.
(23) Fischbach, M. A.; Lin, H.; Liu, D. R.; Walsh, C. T. How Pathogenic Bacteria Evade Mammalian Sabotage in the Battle for Iron. *Nat. Chem. Biol.* **2006**, *2* (3), 132−138.
(24) Piro, N. A.; Robinson, J. R.; Walsh, P. J.; Schelter, E. J. The Electrochemical Behavior of Cerium(III/IV) Complexes: Thermodynamics, Kinetics and Applications in Synthesis. *Coord. Chem. Rev.* **2014**, *260*, 21−36.
(25) Shannon, R. D. Revised Effective Ionic Radii and Systematic Studies of Interatomie Distances in Halides and Chaleogenides. *Acta Crystallogr., Sect. A: Cryst. Phys., Diffr., Theor. Gen. Crystallogr.* **1976**, *A32*, 751−767.
(26) Nakagawa, T.; Mitsui, R.; Tani, A.; Sasa, K.; Tashiro, S.; Iwama, T.; Hayakawa, T.; Kawai, K. A Catalytic Role of XoxF1 as La3+-Dependent Methanol Dehydrogenase in Methylobacterium Extorquens Strain AM1. *PLoS One* **2012**, *7* (11), No. e50480.
(27) Martinez-Gomez, N. C.; Vu, H. N.; Skovran, E. Lanthanide Chemistry: From Coordination in Chemical Complexes Shaping Our Technology to Coordination in Enzymes Shaping Bacterial Metabolism. *Inorg. Chem.* **2016**, *55* (20), 10083−10089.
(28) Cotruvo, J. A., Jr. The Chemistry of Lanthanides in Biology: Recent Discoveries, Emerging Principles, and Technological Applications. *ACS Cent. Sci.* **2019**, *5* (9), 1496−1506.
(29) Pol, A.; Barends, T. R. M.; Dietl, A.; Khadem, A. F.; Eygensteyn, J.; Jetten, M. S. M.; Op den Camp, H. J. M. Rare Earth Metals Are Essential for Methanotrophic Life in Volcanic Mudpots. *Environ. Microbiol.* **2014**, *16* (1), 255−264.
(30) Cotruvo, J. A., Jr.; Featherston, E. R.; Mattocks, J. A.; Ho, J. V.; Laremore, T. N. Lanmodulin: A Highly Selective Lanthanide-Binding Protein from a Lanthanide-Utilizing Bacterium. *J. Am. Chem. Soc.* **2018**, *140* (44), 15056−15061.
(31) Cook, E. C.; Featherston, E. R.; Showalter, S. A.; Cotruvo, J. A., Jr. Structural Basis for Rare Earth Element Recognition by *Methylobacterium Extorquens* Lanmodulin. *Biochemistry* **2019**, *58* (2), 120−125.
(32) Schroll, C. A.; Lines, A. M.; Heineman, W. R.; Bryan, S. A. Absorption Spectroscopy for the Quantitative Prediction of Lanthanide Concentrations in the 3LiCl−2CsCl Eutectic at 723 K. *Anal. Methods* **2016**, *8* (43), 7731−7738.
(33) Grimes, T. S.; Heathman, C. R.; Jansone-Popova, S.; Ivanov, A. S.; Roy, S.; Bryantsev, V. S.; Zalupski, P. R. Influence of a Heterocyclic Nitrogen-Donor Group on the Coordination of Trivalent Actinides and Lanthanides by Aminopolycarboxylate Complexants. *Inorg. Chem.* **2018**, *57* (3), 1373−1385.
(34) Mattocks, J. A.; Ho, J. V.; Cotruvo, J. A., Jr. A Selective, Protein-Based Fluorescent Sensor with Picomolar Affinity for Rare Earth Elements. *J. Am. Chem. Soc.* **2019**, *141* (7), 2857−2861.
(35) Johnson, S. G. NIST46 https://www.nist.gov/srd/nist46 (accessed 2019-08-19).
(36) Kim, H. J.; Eichinger, A.; Skerra, A. High-Affinity Recognition of Lanthanide(III) Chelate Complexes by a Reprogrammed Human Lipocalin 2. *J. Am. Chem. Soc.* **2009**, *131* (10), 3565−3576.
(37) Haiech, J.; Klee, C. B.; Demaille, J. G.; Haiech, J. Effects of Cations on Affinity of Calmodulin for Calcium: Ordered Binding of Calcium Ions Allows the Specific Activation of Calmodulin-Stimulated Enzymes. Theoretical Approach to Study of Multiple Ligand Binding to a Macromolecule. *Biochemistry* **1981**, *20* (13), 3890−3897.
(38) Calisti, L.; Trabuco, M. C.; Boffi, A.; Testi, C.; Montemiglio, L. C.; des Georges, A.; Benni, I.; Ilari, A.; Taciak, B.łło.; Białasek, M.; Rygiel, T.; Krol, M.; Baiocco, P.; Bonamore, A. Engineered Ferritin for Lanthanide Binding. *PLoS One* **2018**, *13* (8), No. e0201859.
(39) Harris, W. R. Binding Constants for Neodymium(III) and Samarium(III) with Human Serum Transferrin. *Inorg. Chem.* **1986**, *25* (12), 2041−2045.
(40) Harris, W. R.; Chen, Y. Difference Ultraviolet Spectroscopic Studies on the Binding of Lanthanides to Human Serum Transferrin. *Inorg. Chem.* **1992**, *31* (24), 5001−5006.

https://dx.doi.org/10.1021/acs.inorgchem.0c01303
Inorg. Chem. 2020, 59, 11855−11867

(41) Aisen, P.; Leibman, A.; Zweier, J. Stoichiometric and Site Characteristics of the Binding of Iron to Human Transferrin. *J. Biol. Chem.* **1978**, *253* (6), 1930−1937.
(42) Allred, B. E.; Rupert, P. B.; Gauny, S. S.; An, D. D.; Ralston, C. Y.; Sturzbecher-Hoehne, M.; Strong, R. K.; Abergel, R. J. Siderocalin-Mediated Recognition, Sensitization, and Cellular Uptake of Actinides. *Proc. Natl. Acad. Sci. U. S. A.* **2015**, *112* (33), 10342−10347.
(43) Nitz, M.; Sherawat, M.; Franz, K. J.; Peisach, E.; Allen, K. N.; Imperiali, B. Structural Origin of the High Affinity of a Chemically Evolved Lanthanide-Binding Peptide. *Angew. Chem., Int. Ed.* **2004**, *43* (28), 3682−3685.
(44) Martin, L. J.; Hähnke, M. J.; Nitz, M.; Wöhnert, J.; Silvaggi, N. R.; Allen, K. N.; Schwalbe, H.; Imperiali, B. Double-Lanthanide-Binding Tags: Design, Photophysical Properties, and NMR Applications. *J. Am. Chem. Soc.* **2007**, *129* (22), 7106−7113.
(45) Tinoco, A. D.; Saxena, M.; Sharma, S.; Noinaj, N.; Delgado, Y.; Quiñones González, E. P.; Conklin, S. E.; Zambrana, N.; Loza-Rosas, S. A.; Parks, T. B. Unusual Synergism of Transferrin and Citrate in the Regulation of Ti(IV) Speciation, Transport, and Toxicity. *J. Am. Chem. Soc.* **2016**, *138* (17), 5659−5665.
(46) Jensen, M. P.; Gorman-Lewis, D.; Aryal, B.; Paunesku, T.; Vogt, S.; Rickert, P. G.; Seifert, S.; Lai, B.; Woloschak, G. E.; Soderholm, L. An Iron-Dependent and Transferrin-Mediated Cellular Uptake Pathway for Plutonium. *Nat. Chem. Biol.* **2011**, *7* (8), 560−565.
(47) Park, D. M.; Brewer, A.; Reed, D. W.; Lammers, L. N.; Jiao, Y. Recovery of Rare Earth Elements from Low-Grade Feedstock Leachates Using Engineered Bacteria. *Environ. Sci. Technol.* **2017**, *51* (22), 13471−13480.
(48) Park, D.; Middleton, A.; Smith, R.; Deblonde, G.; Laudal, D.; Theaker, N.; Hsu-Kim, H.; Jiao, Y. A Biosorption-Based Approach for Selective Extraction of Rare Earth Elements from Coal Byproducts. *Sep. Purif. Technol.* **2020**, *241*, 116726.
(49) Taggart, R. K.; Hower, J. C.; Dwyer, G. S.; Hsu-Kim, H. Trends in the Rare Earth Element Content of U.S.-Based Coal Combustion Fly Ashes. *Environ. Sci. Technol.* **2016**, *50* (11), 5919−5926.
(50) Martin, L. J.; Sculimbrene, B. R.; Nitz, M.; Imperiali, B. Rapid Combinatorial Screening of Peptide Libraries for the Selection of Lanthanide-Binding Tags (LBTs). *QSAR Comb. Sci.* **2005**, *24* (10), 1149−1157.
(51) Dautry-Varsat, A.; Ciechanover, A.; Lodish, H. F. pH and the Recycling of Transferrin during Receptor-Mediated Endocytosis. *Proc. Natl. Acad. Sci. U. S. A.* **1983**, *80* (8), 2258−2262.
(52) Correnti, C.; Strong, R. K. Mammalian Siderophores, Siderophore-Binding Lipocalins, and the Labile Iron Pool. *J. Biol. Chem.* **2012**, *287* (17), 13524−13531.
(53) Park, D. M.; Reed, D. W.; Yung, M. C.; Eslamimanesh, A.; Lencka, M. M.; Anderko, A.; Fujita, Y.; Riman, R. E.; Navrotsky, A.; Jiao, Y. Bioadsorption of Rare Earth Elements through Cell Surface Display of Lanthanide Binding Tags. *Environ. Sci. Technol.* **2016**, *50* (5), 2735−2742.
(54) Brewer, A.; Dohnalkova, A.; Shutthanandan, V.; Kovarik, L.; Chang, E.; Sawvel, A. M.; Mason, H. E.; Reed, D.; Ye, C.; Hynes, W. F.; Lammers, L. N.; Park, D. M.; Jiao, Y. Microbe Encapsulation for Selective Rare-Earth Recovery from Electronic Waste Leachates. *Environ. Sci. Technol.* **2019**, *53* (23), 13888−13897.
(55) Uversky, V. N. Intrinsically Disordered Proteins and Their "Mysterious" (Meta)Physics. *Front. Phys.* **2019**, *7*, 10.
(56) Binnemans, K.; Jones, P. T.; Blanpain, B.; Van Gerven, T.; Yang, Y.; Walton, A.; Buchert, M. Recycling of Rare Earths: A Critical Review. *J. Cleaner Prod.* **2013**, *51*, 1−22.

https://dx.doi.org/10.1021/acs.inorgchem.0c01303
Inorg. Chem. 2020, 59, 11855−11867